Available online at www.sciencedirect.com
ScienceDirect
Vision Research 47 (2007) 50–59
Vision Research
www.elsevier.com/locate/visres

Spatially asymmetric response to moving patterns in the visual cortex: Re-examining the local sign hypothesis

David Whitney [a,b,*], David W. Bressler [a]

[a] The Center for Mind and Brain, The University of California, Davis, CA 95616, USA
[b] The Department of Psychology, The University of California, Davis, CA 95616, USA

Received 15 June 2006; received in revised form 11 August 2006

Abstract

One of the most fundamental functions of the visual system is to code the positions of objects. Most studies, especially those using fMRI, widely assume that the location of the peak retinotopic activity generated in the visual cortex by an object is the position assigned to that object—this is a simplified version of the local sign hypothesis. Here, we employed a novel technique to compare the pattern of responses to moving and stationary objects and found that the local sign hypothesis is false. By spatially correlating populations of voxel responses to different moving and stationary stimuli in different positions, we recovered the modulation transfer function for moving patterns. The results show that the pattern of responses to a moving object is best correlated with the response to a static object that is located behind the moving one. The pattern of responses across the visual cortex was able to distinguish object positions separated by about 0.25 deg visual angle, equivalent to approximately 0.25 mm cortical distance. We also found that the position assigned to a pattern is not simply dictated by the peak activity—the shape of the luminance envelope and the resulting shape of the population response, including the shape and skew in the response at the edges of the pattern, influences where the visual cortex assigns the object's position. Therefore, visually coded position is not conveyed by the peak but by the overall profile of activity.

Keywords: Vision; Perception; Motion; Motion perception; fMRI; Retinotopy; Topography; Local sign; Localization; Labeled line; Visual cortex; Striate cortex

1. Introduction

Visual information is coded topographically in many early visual areas. This retinotopy is generally agreed upon to be fundamental to visual processing and may underlie the visual system's ability to make precise discriminations of object position, bind features, and localize objects (Lennie, 1998). Despite the prevalence of retinotopy throughout the cortex, it remains unclear what exactly counts as a retinotopically coded position—what is the relevant information carried by a neuron or population of neurons that determines the perceived location of an object?

The most common assumption, especially in the human neuroimaging literature, is the idea of local signs, where the *peak response* to a stimulus in the visual cortex is taken as the coded location of the object. (By peak response, we mean the peak BOLD response, which is commonly believed to reflect population-level neuronal activity.) Although this seems oversimplified, there has been a long-standing debate in the psychophysics literature over this question; perceived location could be determined by peak contrast (Hess & Holliday, 1992) or zero crossings in the luminance distribution (Watt & Morgan, 1983). However, most of the recent psychophysical results strongly suggest that perceived position does not simply depend on peak contrast or intensity alone (Morgan, Mather, Moulden, & Watt, 1984; Regan, 2000; Whitaker, McGraw, & Levi, 1997). Rather, the contrast distribution (e.g., weighted mean or centroid of a pattern) determines perceived position (Watt, Morgan, & Ward, 1983; Westheimer & McKee, 1977a; Whitaker, McGraw, Pacey, & Barrett,

* Corresponding author. Fax: +1 5307921489.
E-mail address: dwhitney@ucdavis.edu (D. Whitney).

0042-6989/$ - see front matter © 2006 Elsevier Ltd. All rights reserved.
doi:10.1016/j.visres.2006.08.030

1996). Therefore, how could peak responses in the visual cortex carry enough information to adequately convey positional information? Despite the psychophysical evidence that prompts this question, it remains unclear what the position code is in human visual cortex; most neuroimaging studies still report the locations of peak activity, either visually (e.g., color-coded maps of retinotopy) or in standardized space such as Talairach or Montreal Neurological Institute (MNI) coordinates (Collins, Neelin, Peters, & Evans, 1994; Talairach & Tournoux, 1988). A great number of imaging studies on human visual cortex are therefore implicitly or explicitly based on the premise of local signs.

Two recent imaging studies began to approach this issue, showing that there is a spatially asymmetric BOLD response to moving patterns; specifically, there is a stronger response at the trailing edges of moving objects (Koyama, Sasaki, Watanabe, & Tootell, 2003; Whitney et al., 2003). However, these studies were not designed to address the question of local signs. The coded location of the moving object may perhaps be determined entirely by the peak response while the population of active voxels (reflecting populations of neuronal activity) simultaneously shows a spatial asymmetry (Ashida & Smith, 2005; Liu, Ress, Nakadomari, & Wandell, 2004). If the peak response is the most relevant information for determining retinotopically coded location, then a spatial asymmetry in the response due to visual motion may not be detected by the visual cortex as a change in the coded location. Therefore, an open and fundamental question remains: how is position assigned in the visual cortex? Is the coded location of an object (i.e., the location that determines our percept of an object's position) determined by the peak response alone? If perceived position is determined by local signs, then what is the local sign? Is it the peak response to a stimulus, the edges of the response, or the entire shape of the population response?

The goals of the following experiments are twofold. First, we develop a new and extremely sensitive technique for measuring the retintopically coded location of an object to address whether visual motion shifts or skews the spatial pattern of activity in the visual cortex. This will address a recent debate over the coding of moving objects in the visual cortex. Second, and more importantly, we will critically examine the notion that a local sign (the coded location of an object) simply corresponds to the peak response in the visual cortex. We will show that, contrary to the common assumption, the peak response in the visual cortex is not sufficient to explain the coded location of an object. Rather, the entire pattern of responses carries meaningful information about object position.

2. Methods

Six subjects participated in the first functional imaging experiment; four of these six subjects participated in the second experiment. Scanning protocols were approved by the University of California, Davis, Human Subject Review Board. Imaging was conducted on a 3-T Siemens TRIO scanner located at the UC Davis Imaging Research Center. Each participant's head was rested in a Siemens eight-channel phased-array head coil. Braces and padding on the side and forehead of the participant restricted head motion and provided feedback to the subject about any potential body movements. Stimuli were back-projected with a projector (75 Hz) onto a semi-transparent screen from outside the bore. A mirror located 7.5 cm directly above the subject provided a reflected view of the stimuli. Subjects fixated on a bull's-eye at the center of the screen at all times. Functional images were acquired with a gradient-recalled echo EPI sequence. Whole-brain structural images were collected with a high resolution (1 mm^3) Turbo Spin Echo scan that was used to align functional images. The acquisition parameters were: TR = 2000 ms, TE = 26 ms, FA = 90 deg, FOV = 22×22 cm^2, voxel size = $1.528 \times 1.528 \times 2.5$ mm^3, 20 slices per volume. The imaging volume was parallel to and centered on the calcarine sulcus, covering the occipital lobe (Fig. 1C).

2.1. Experiment 1

2.1.1. Localizer runs

There were five conditions in the localizer, along with one fixation baseline condition, for a total of six conditions. In each of the five experimental conditions, four counterphase flickering Gabors were presented centered on an iso-eccentric circle around the fixation point; the eccentricity of the four Gabors could be 10.51, 10.73, 10.89 (central condition), 11.21, or 11.64 deg (Fig. 1). Relative to the central condition, the five Gabors were separated by −0.38, −0.16, 0, 0.32, or 0.75 deg, respectively. Negative values indicate that the Gabors were more foveal and positive values indicate that the Gabors were more eccentric, relative to the central condition. Each Gabor was formed by multiplying a sinusoidal luminance modulation by a Gaussian contrast envelope to blur the edges, which provides a means of displacing the stimuli in sub-pixel increments when necessary (Morgan et al., 1984). Each Gabor was 0.32 cyc/deg, 7.5 Hz, and 85% Michelson contrast. The Gaussian contrast envelope of each Gabor was defined as $L(x,y) = A\{\exp[-r^2/(\sigma M)^2]\}$, where A is the peak contrast amplitude, r is the distance of (x,y) from the center of the Gaussian, σ is standard deviation, and M is the maximum radius. On each trial (each 10 s block) the phase of each Gabor was randomized. Stimuli were presented in a standard blocked design. Each run consisted of 30 ten-second blocks. The six conditions were randomly interleaved. Each subject participated in four to seven functional localizer runs.

For each functional run, a general linear model (GLM) was conducted with five predictors (corresponding to the five Gabor positions). Separate functional maps were computed using each of the five Gabors as a contrast in the GLM. For example, the condition in which the Gabors were located at 10.51 deg eccentricity was compared to the fixation baseline; a similar contrast was repeated for each of the other four Gabor eccentricities. This resulted in five separate volumetric functional maps. In these three-dimensional maps, every voxel has a statistical value associated with it (there is no threshold—each voxel has a t value, though many are very close to zero). In a separate GLM, all five Gabor locations were compared to the fixation baseline (giving a union of responses to all five Gabor locations). This was used as a conservative localizer covering all of primary visual cortex—a region of interest (ROI; Fig. 1C). In separate analyses, we confirmed that the overall size of the ROI (the statistical threshold used to determine the extent of the ROI) did not affect the results. We also confirmed that selecting this ROI from the segmented cortical surface of each subject (Fig. 1C, right panel, excluding white matter) did not alter the pattern of results.

2.1.2. Experimental runs

The experimental stimuli consisted of the same four Gabor patterns located at 10.89 deg eccentricity (the same eccentricity as the central condition in the localizer runs). The difference in the experimental runs was that the Gabors contained unidirectional motion either toward or away from the fovea (4.8 Hz, Fig. 1, bottom panel). There were three conditions in the experiment. In one condition, the four Gabors contained contracting motion (motion toward the fovea), and in another condition

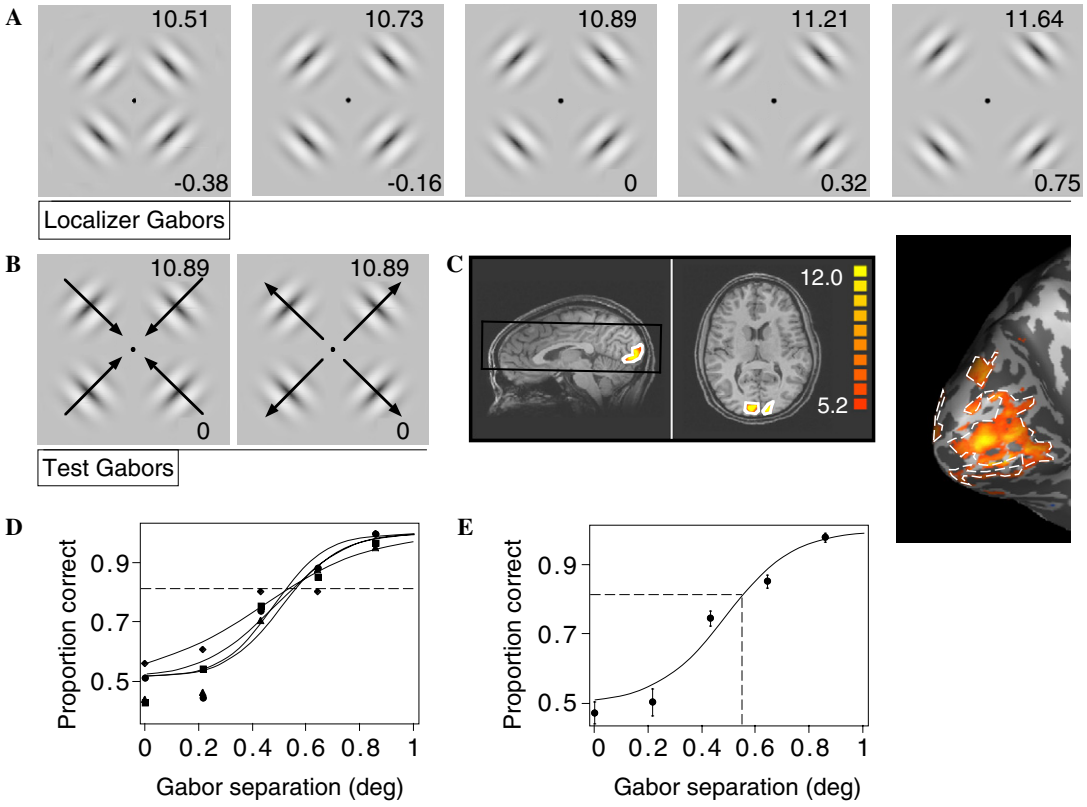

Fig. 1. Localizer and experimental stimuli used in the first experiment. (A) Localizer stimuli consisted of a set of four Gabor patterns (sinusoidal luminance carriers with a Gaussian contrast envelope) presented at one of five possible eccentricities (upper right corner of each image). The carriers of each Gabor were flickered in counterphase at 7.5 Hz. (B) Experimental stimuli consisted of the exact same Gabor patterns presented at 10.89 deg eccentricity (the same as one of the localizer conditions). The number on the bottom right of each localizer stimulus in (A) indicates the distance between the localizer and experimental Gabors. The only difference with the experimental Gabors was that the sinusoidal luminance carrier drifted either toward or away from the fovea (rather than being static). The physical and retinal locations of the drifting Gabors were identical to one of the localizer conditions. (C) The slice plan (black rectangle) and region of interest (ROI) for one representative subject. An ROI (white circled regions on volumetric and surface maps, t values at right, $P < 0.01$ Bonferroni corrected) was defined separately for each subject as the union of all voxels that responded to any of the localizer Gabors; this conservatively encompassed all of the voxels in the visual cortex that respond to the Gabors and ensured that few voxels were left out of the analysis. (D) Psychophysical results for four subjects. A two-interval forced choice experiment measured the discriminability of the five Gabor conditions. All four subjects had consistent 83% discrimination thresholds. (E) The mean threshold discrimination across subjects was ~0.55 deg. There was a significant difference between the discriminability of Gabors separated by less than 0.4 deg (Wilcoxon signed ranks test, $Z = -2.03$, $P < 0.05$, two tailed). The results indicate that subjects were able to perceptually discriminate between the different localizer conditions.

the same Gabors contained expanding motion (outward motion, away from the fovea). A third condition consisted of a fixation baseline. The Gabors themselves, the design of the experimental runs, and the procedure were identical to those in the localizer.

For each functional run, a general linear model (GLM) was fit to the data with two predictors corresponding to the two Gabor directions of motion. Separate functional maps were computed using each of the moving Gabors as a contrast in the GLM (inward or outward motion). For example, the condition in which the Gabors contained inward motion was compared to the fixation baseline; a similar contrast was repeated for outward motion. This resulted in two separate volumetric functional maps similar to those above, but for drifting rather than flickering stimuli.

2.1.3. Attention task

In all functional runs (both localizer and experimental runs), subjects performed a difficult task at the fixation point. A small monochromatic pattern was intermittently presented superimposed on the fixation point. The pattern could be high or low spatial frequency and was presented approximately 10 times during each 10-s block. Subjects were instructed to count the number of high and low spatial frequency patterns and by the end of the 10 s block report whether more high or low spatial frequency patterns had been presented. Without accurate fixation, the task was impossible, ensuring that subjects attended and fixated at the screen center throughout each run.

2.1.4. Analysis

All preprocessing, including linear trend removal and 3D motion correction, as well as GLM analyses (above) were conducted with Brain Voyager QX (Brain Innovation B.V., Maastricht, The Netherlands). The images were not spatially smoothed. A correction for serial correlations (removal of first-order autocorrelation) was used prior to all GLM analyses.

All correlational analyses (cf. Haxby et al., 2001) were conducted with Matlab (The Mathworks, Natick, Massachusetts). Within the ROI (Fig. 1C) of each subject, each of the five functional localizer maps was cross-correlated with the two functional experimental maps (5 localizer Gabor eccentricities × 2 directions of motion = 10 correlations). The cross-correlation was repeated for each functional run, and each of these 10 cross-correlation (r) values was converted to Fisher's z values and averaged within condition across runs (Cohen, 1988). This resulted in 10 averaged Fisher's z scores, which gives an indication of the retinotopic correlation in the population response to the drifting and flickering Gabors (Fig. 3). (Here, we use the term population response to refer to a collection of voxels; voxels, in turn, are generally thought to reflect

the responses of populations of neurons.) The physical (retinal) eccentricity of the drifting Gabors was 10.89 deg, so the population response to these Gabors should best correlate with the localizer Gabors that are also located at 10.89 deg. Any difference in this peak correlation between the moving Gabors and the localizer Gabors reveals a shift in the representation of the drifting Gabors (e.g., if the drifting Gabors at 10.89 deg eccentricity correlate best with localizer Gabors at 11.64 deg). The significance of each correlation and differences between each correlation were estimated by comparing Fisher's z scores (Alexander, Scozzaro, & Borodkin, 1989) both within and between subjects, as well as using bootstrapping and shuffling procedures (Efron & Tibshirani, 1993). In the bootstrap technique, 10,000 subsamples of the test correlation (voxels from the ROI in, e.g., Fig. 2) were repeatedly drawn (resampled with replacement) and correlated; only if the frequency distribution showed no subsamples close to zero ($P < 0.0001$) was the correlation considered significant. In the shuffling procedure, the pairwise voxel values (t scores) in the test correlation (e.g., Fig. 2) were randomly shuffled and re-correlated. This was repeated 10,000 times. The test correlation was considered significant if the entire frequency distribution of shuffled correlations fell near 0 and no random correlation fell near the test correlation ($P < 0.0001$). In a final statistical control measure, we redefined each cross-correlation (e.g., Fig. 2) using Spearman's rho and ensured that the results did not differ using nonparametric methods.

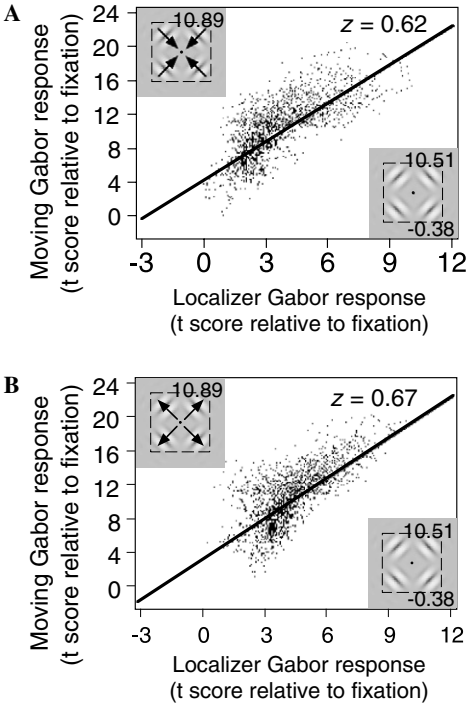

Fig. 2. Sample correlation between the population response generated by one localizer condition (at 10.51 deg) and the experimental drifting Gabors. (A) The abscissa shows the result of a GLM analysis in which the localizer Gabors were compared to fixation baseline; each voxel has a statistical t value associated with it—higher values indicate that the voxel strongly responded to the localizer Gabors. The ordinate shows the resulting t values for a GLM analysis in which either the inward or outward drifting Gabors were compared to the fixation baseline; higher t values indicate that the voxel responded strongly to the drifting Gabors. The correlation between responses to the localizer and drifting Gabors is computed across the entire set of voxels defined in the ROI. The correlation between the population activity generated by the localizer and the inward drifting Gabors was $z = 0.62$ (equivalent Fisher's z transformed from r values). (B) The correlation between the localizer and the outward drifting Gabors was $z = 0.67$. The physical and retinal distance between the localizer Gabors and both the inward and outward drifting Gabors was the same. There should therefore have been no difference in the correlation between localizer Gabors and the two drifting Gabors. However, there was a significant difference: the population response to the more foveal localizer Gabors correlated better with the population response to the outward drifting Gabors (Fisher's z comparison; $Z = 2.9$, $P < 0.01$).

2.2. Experiment 2

The second experiment was identical in all respects to the first experiment except the localizer Gabors were modified slightly. Rather than shifting the Gabors to one of five different eccentricities, we skewed the contrast envelopes of the Gabors while leaving the peak contrast at the same eccentricity of 10.89 deg (Fig. 5), the same eccentricity of the drifting Gabors. As in the first experiment, there were five localizer Gabor conditions; the central condition (Fig. 5C) was identical to that in the first experiment (standard deviation of the Gabor's envelope was 2.1 deg symmetrically), while the other four conditions had Gabors with contrast envelopes that were skewed inward or outward. To skew the Gabors, the standard deviation of the central and peripheral halves of each Gabor was independently varied; that is, each half of the abutting Gabor had a different standard deviation while the location at which the two halves met was constant and always defined the peak contrast (Whitaker et al., 1997, 1996). In the no-skew condition (identical to Experiment 1), the standard deviation was ~2.1 deg on both halves of the Gabor (Fig. 5C). The Gabors that were most skewed toward the fovea had a standard deviation that was increased by 0.46 deg toward the fovea and decreased by 0.45 deg in the periphery (for a net skew of 0.92 deg). The second most skewed Gabors (Fig. 5B) had envelopes increased and decreased by 0.23 and 0.23 deg in their central and peripheral halves, respectively (for a net skew of 0.46 deg). The Gabors in Fig. 5D and E were skewed peripherally and had envelopes that were mirror symmetrical to those in Fig. 5A and B.

In a separate psychophysical experiment, we measured the discriminability of the five Gabor conditions. The stimuli were identical to those in Experiment 1 (Fig. 1). Four of the subjects from Experiment 1 participated in this experiment, which was conducted in a dark, soundproof experimental chamber. The reason for collecting psychophysical data separately from the imaging experiment was because in the imaging experiment we wanted to control for attention as precisely as possible across conditions. The attention task in the imaging experiments was therefore presented at the fovea, preventing subjects from reporting the relative positions of the Gabors. In the psychophysical experiment, subjects were seated 40 cm from a Sony G520 Multiscan CRT monitor. In each trial, one of the conditions (in Fig. 1A) was presented for 500 ms, followed by a second interval (500 ms) in which either the same or a different condition was presented. In a method of constant stimuli, two-interval forced choice discrimination, subjects judged which interval contained more eccentric Gabors. Cumulative response accuracy was plotted as a function of Gabor separation (the difference in eccentricity between the stimuli in the two intervals), and a logistic function was fit to the data. The logistic function was expressed as:

$$f(x) = [1/(2 + \exp[\alpha(x + \beta)]) + 0.5]$$

where parameter (α) was the slope and (β) is the 83% correct threshold. There were five conditions (five Gabor eccentricities) and 20 trials per condition. Each subject participated in three sessions, for a total of 300 trials.

3. Results

Experiment 1 had two components, localizer runs and separate experimental runs (see Section 2). Localizer stimuli consisted of a set of four flickering Gabor patterns presented at one of five possible eccentricities (Fig. 1A); we

confirmed that subjects were able to psychophysically distinguish these five different localizer Gabor conditions (Fig. 1D–E). In the experimental runs, a set of four drifting Gabors was always in the same location (10.89 deg eccentricity) but contained expanding or contracting motion (Fig. 1B). The goal was to spatially correlate activation produced by the localizer and experimental Gabors across the visual cortex (Fig. 1C). We expected the spatial correlation to vary depending on the retinotopic distance between the stimuli.

Fig. 2A shows an example correlation between the flickering localizer Gabors located at 10.51 deg eccentricity and the inward drifting Gabors. Fig. 2B shows the correlation between the same flickering localizer Gabors and the outward drifting Gabors. In these cases, the localizer Gabors were located 0.38 deg more foveally than both drifting Gabors (expanding and contracting conditions). Interestingly, in this case, there was a significantly higher spatial correlation for the outward than the inward motion condition ($Z = 2.9$, $P < 0.01$, Fisher's z comparison, Alexander et al., 1989).

Fig. 3A shows each of the ten cross-correlation values for one representative subject. The population responses to the flickering localizer Gabors that are more eccentric correlate better with the population responses to the inward drifting Gabors (white symbols). For example, the flickering Gabors at 11.64 deg (0.75 deg more peripheral than the drifting Gabors) correlated better with the inward drifting Gabors by ~0.17 Fisher's z units ($Z = 9.8$, $P < 0.001$). Because the eccentricity of both inward and outward drifting Gabors was always the same, there should have been no difference in the correlation as a function of motion direction (the black and white data curves should have overlapped). However, it is clear that there is a spatial bias.

To quantify the spatial shift in the peak correlation across all six subjects, we fit a Gaussian to the data representing each direction of motion in Fig. 3B. The difference in the two best-fit Gaussians reveals a ~0.24 deg shift in the peak correlation for inward versus outward moving Gabors (dashed and solid curves, respectively). That is, Gabors that contain directional motion produce population responses that better correlate with static patterns that are physically located (i.e., shifted) in a position opposite the direction of the drifting Gabors' motion. The shift required for optimal correlation is small, but significant ($F_{(4,20)} = 11.4$, $P < 0.001$). The amplitude and standard deviation of the fitted Gaussians differs slightly for inward versus outward motion, but this did not influence the fact that the peak correlation was shifted along the X-axis: when we fixed the amplitude and standard deviation of the fitted Gaussians while leaving only the position of the peak correlation as a free parameter, the 0.24 deg shift remained. Fig. 3C shows the net effect of motion on the representation of position (the difference in Fisher's z scores from Fig. 3B). The negative slope indicates that drifting Gabors better correlate with flickering Gabors that

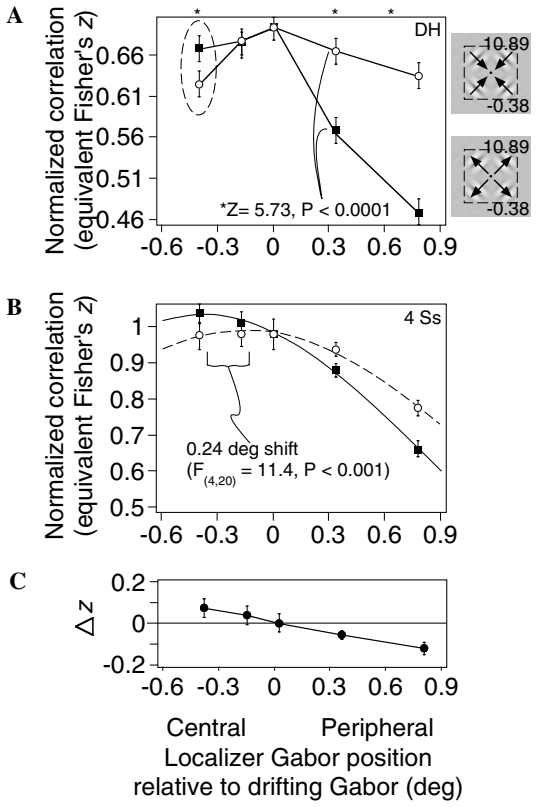

Fig. 3. The cross correlation between all localizer and experimental Gabor conditions. (A) Results for one representative subject. The abscissa shows the relative position of the localizer and experimental Gabors: a value of 0 indicates that the flickering localizer Gabors were presented at the same eccentricity as the drifting Gabors; positive and negative values indicate that the localizer Gabors were more eccentric or foveal, respectively, than the drifting Gabors. Gabors containing inward and outward motion are indicated by white and black symbols, respectively. The ordinate shows the correlation for each pair of conditions (calculated as in Fig. 2); the pair of correlations from Fig. 2 is circled with a dashed line. It is clear that the inward drifting Gabors (white symbols) produced a population-level response that tended to correlate better with the response to the more eccentric flickering Gabors. Conversely, the outward drifting Gabors (black symbols) correlated better with the more foveal localizer Gabors. Asterisks at the top of the graph indicate that the pairwise differences between the correlations were significant (Fisher's z comparison, Bonferroni corrected, $P < 0.01$). (B) Results for all six subjects. The cross-correlations (Fisher's z values) were averaged and a Gaussian function $f(x)=\{a \cdot \exp[-(x+c)^2]/(b^2)\}$ was fit to the data, where a is the amplitude, b is the standard deviation, and c is the position of the peak. The best-fit parameters for the inward moving Gabors (dashed curve, $r^2 = 0.99$) were $a = 0.991$, $b = 3.173$, and $c = 0.256$. The best-fit parameters for the outward moving Gabors (solid curve, $r^2 = 0.99$) were $a = 1.035$, $b = 2.89$, and $c = 0.630$. The difference in the position of the peak correlation (c) for inward versus outward moving Gabors is 0.24 deg. This indicates that drifting patterns produced a population level response that was better characterized by a static pattern whose location was shifted in the opposite direction. The difference (i.e., the interaction) between the two curves is significant ($F_{(4,20)} = 11.4$, $P < 0.001$). (C) The net effect of visual motion on the representation of position as revealed by the population activity. For each localizer Gabor position (abscissa), the difference in the Fisher's z scores for outward minus inward moving Gabors is plotted (from B). The negative slope in the data indicates that drifting patterns better correlated with flickering localizer Gabors that were shifted in the opposite direction (Friedman test, $X^2_{(4)} = 21.2$, $P < 0.0001$). There is a significant difference in the effect for Gabors as closely spaced as −0.38 deg versus 0 deg. (Wilcoxon signed rank test, $Z = 2.3$, $P < 0.05$). Error bars ± SEM.

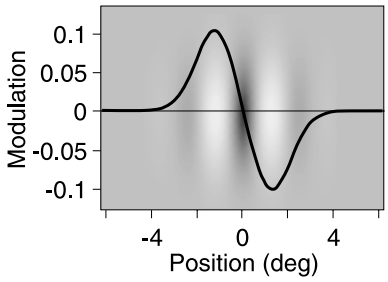

Fig. 4. The modulation transfer function for moving patterns, with a superimposed Gabor that contains rightward motion. The location of the static localizer Gabor that yielded the peak correlation in the population response was shifted ~0.12 deg from the rightward drifting Gabor (interpolated based on the 0.24 deg shift in the best-fit Gaussian in Fig. 3B). Deconvolving the physical position of the rightward drifting Gabor with the position of the optimally shifted static localizer Gabor revealed a spatially biphasic modulation transfer function (black curve). The relative size of this kernel, compared to the size of the drifting Gabor, is indicated by the superimposed image of the Gabor (whose full width at half maximum amplitude was ~4.9 deg). The peak modulation occurs near the edges of the Gabor, where the contrast envelope drops off.

were physically shifted in the opposite direction (Friedman test, $X^2_{(4)} = 21.2$, $P < 0.0001$).

The peak correlation for the inward moving Gabors (always at 10.89 deg eccentricity) occurs for static flickering Gabors located at ~11.2 deg eccentricity (Fig. 3B). Deconvolving this optimally correlated Gabor with the physical location of the drifting Gabor reveals a modulation transfer function (Fig. 4). Interestingly, this convolution kernel operates over a very large scale (>5 deg) and is spatially biphasic. Note that the positive and negative lobes in the modulation transfer function do not necessarily correspond to excitation and inhibition but refer to the modulation in the BOLD response, and because both excitation and inhibition may contribute to the BOLD response (Attwell & Iadecola, 2002; Caesar, Gold, & Lauritzen, 2003; Harel, Lee, Nagaoka, Kim, & Kim, 2002; Mathiesen, Caesar, Akgoren, & Lauritzen, 1998; Thomsen, Offenhauser, & Lauritzen, 2004; Waldvogel et al., 2000), our results do not discriminate which generates positive or negative modulation.

The results above show that moving patterns produce a population response that is equivalent to a shift in the location of the pattern. Although this demonstrates a sensitivity to retinotopic shifts, the question remains whether the peak response to a stimulus is the only relevant information coded by the visual cortex when assigning object location. Psychophysical evidence has long suggested that the shape of an object's contrast envelope does influence perceived position (Morgan et al., 1984; Regan, 2000; Whitaker et al., 1997). If retinotopic coding in the visual cortex contributes to perceived position, then we would expect not only the peak response, but the entire shape of the contrast envelope and resulting population response to carry meaningful information about object position. We tested this in Experiment 2 by fixing the location of each flickering localizer Gabor's peak contrast while varying its contrast envelope (Fig. 5); we then correlated these new localizer Gabors with the drifting ones.

Fig. 6 shows the results of the second experiment, in which we correlated the drifting Gabors with static flickering Gabors that had skewed Gaussian contrast envelopes (Fig. 5). Thus, the localizer Gabors were not shifted as in the first experiment, but had distorted contrast profiles; the peak contrast in each Gabor stimulus was at the same eccentricity (10.89 deg). Similar to Fig. 3, there was a shift in the optimal correlation in the population response to moving Gabors ($F_{(4,12)} = 18.8$, $P < 0.001$). Fig. 6A shows the net effect of motion on the representation of position: the inward moving Gabors correlated better with flickering Gabors that were skewed in an eccentric direction. Likewise, the Gabors containing outward motion produced a population response that better correlated with the flickering Gabors that were skewed more foveally (Friedman test, $X^2_{(4)} = 16$, $P < 0.004$). These results, and the modulation transfer function (Fig. 6B), are similar to those revealed in the first experiment. *Population-level* activity in the visual cortex therefore detects alterations in the contrast envelopes of stimuli, even when the peak remains fixed, and uses this information to convey meaningful information about retinotopic position.

4. Discussion

The results here suggest that the topographically organized population response in visual cortex is modulated by visual motion, supporting previous findings. The results also show that the pattern of activity (the population of voxels) is able to distinguish the positions of objects separated by very small displacements. The recovered modulation transfer function suggests that there are long-range mechanisms in early visual cortex. Finally, the results indicate that the location assigned to an object is not dictated by the peak contrast or peak activation; rather, the entire pattern of responses, largely determined by the object's contrast envelope, carries information about coded location.

4.1. Retinotopic distortions

The population response to a visual pattern was modulated when the pattern contained motion: the spatial distribution of activity was shifted or skewed opposite the direction of motion. The two experiments here revealed a similar modulation transfer function for moving patterns, using both shifted and skewed localizer stimuli, providing converging evidence that either a shift or a skew in the contrast envelope of a stimulus produces a noticeable change in the population response. This supports previous psychophysical evidence showing that human observers are able to discriminate the positions of patterns that have differentially skewed contrast envelopes (Morgan et al., 1984; Regan, 2000; Whitaker et al., 1997, 1996). The population-level representation of such patterns in early visual

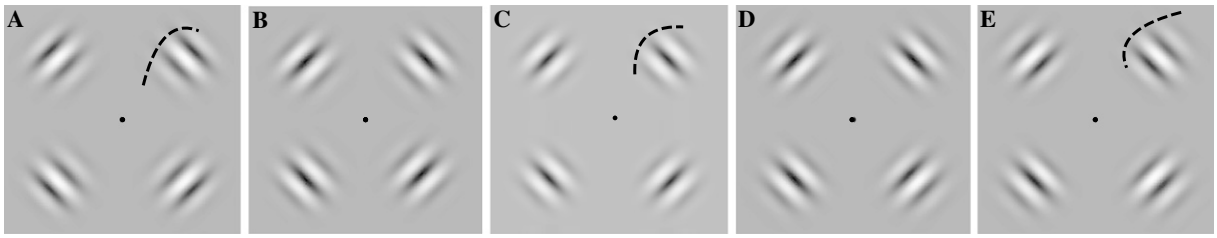

Fig. 5. Localizer stimuli used in the second experiment. (A–E) Rather than using shifted localizer Gabors, the contrast envelopes of the localizer Gabors were skewed: the eccentricity of the peak contrast for all localizer Gabors was identical (10.89 deg), but the standard deviation of the envelope was extended in one direction and foreshortened in the other (roughly indicated by the black dashed lines, which were not visible in the actual stimuli; see Section 2 for details). The Gabors with no skew (C) were identical to the drifting Gabors, except they flickered at 7.5 Hz.

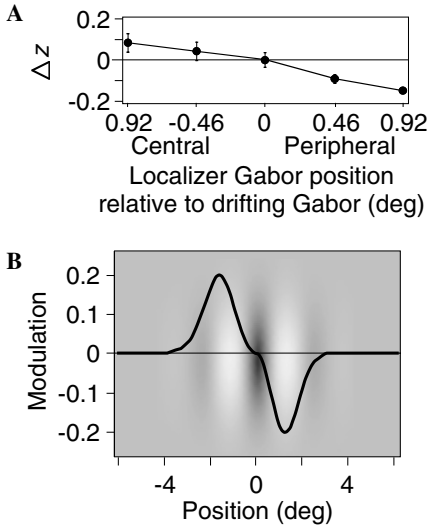

Fig. 6. Results of the second experiment for four subjects. (A) The net change in the population-level correlation between moving and skewed localizer Gabors as a function of the Gabor's motion (same format as Fig. 3C). For each position of the localizer Gabor, positive Δ Fisher's z values along the ordinate indicate that the population correlation was higher for the outward drifting Gabors; negative Δz values indicate that the correlation was higher for the inward drifting Gabors. The negative slope in the data curve indicates that Gabors drifting in one direction better correlate with localizer Gabors that are skewed in the opposite direction ($F_{(4,12)} = 18.8$, $P < 0.001$). (B) The modulation transfer function for a rightward drifting Gabor (obtained by deconvolving the optimally skewed Gabor with the physically presented one). The superimposed Gabor gives an indication of scale. The resulting function is similar to that revealed using shifted localizer Gabors (Fig. 4).

cortical areas may therefore underlie the perceptual discrimination of object position.

The relatively large spatial extent of the modulation transfer function (Figs. 4 and 6) is somewhat surprising given the size of classical receptive fields in V1 (Daniel & Whitteridge, 1961; Hubel & Wiesel, 1962, 1968; Maffei & Fiorentini, 1976). However, long-range horizontal connections and extended surround modulation have been found in V1 (Allman, Miezin, & McGuinness, 1985; Cavanaugh, Bair, & Movshon, 2002; Fitzpatrick, 2000; Gilbert, 1998; Li & Li, 1994). Feedback from MT to V1 (Edelman, 1978; Zeki, 1990) might also play an important role in modulating and perhaps even mediating the perception of an object's location (Durant & Johnston, 2004; McGraw, Walsh, & Barrett, 2004; Nishida & Johnston, 1999; Pascual-Leone & Walsh, 2001; Whitney & Cavanagh, 2000). Feedback may therefore be an important contributor to the large modulation transfer function field found here.

The spatial distribution of activity shifted or skewed opposite the direction of motion. In contrast, many psychophysical studies have shown that objects generally appear shifted in the direction of nearby motion (De Valois & De Valois, 1991; Nishida & Johnston, 1999; Ramachandran & Anstis, 1990; Snowden, 1998; Whitaker, McGraw, & Pearson, 1999); for a review, see (Whitney, 2002). There are several possible mechanisms that could explain this counterintuitive result, including sequential recruitment (McKee & Welch, 1985; Snowden & Braddick, 1989; Verghese & McKee, 2002; Welch, Macleod, & McKee, 1997), deblurring (Burr, Fiorentini, & Morrone, 1998; Burr, Ross, & Morrone, 1986; Whitney et al., 2003), motion sharpening (Bex, Edgar, & Smith, 1995; Hammett, 1997; Hammett & Bex, 1996), attention (Koyama et al., 2003; Verghese & McKee, 2002), and differential adaptation at the trailing and leading edges of the pattern, caused by one of these or another process. Unfortunately, at this point we only know what the shape of the modulation transfer function is for moving objects (Figs. 4 and 6), but we do not know what process is responsible. The resolution of this issue is important, because it may reveal the differential mechanisms that code the positions of moving and stationary objects.

If the current results confirm prior studies, what is the advantage of the spatial correlation technique here? The current analysis was based on *patterns* of BOLD response, whereas the previous studies on the same phenomenon used estimates of BOLD *magnitude*. There are several advantages of the current approach that merit highlighting. First, the patterns of BOLD responses carry extremely precise information. Indeed, the positions of objects separated by less than 0.25 deg could be discriminated with statistical significance. Moreover, this is not the limit of the technique. If stimuli were presented near the fovea, it is conceivable that this technique could reveal discrimination of object representations in the hyperacuity range. Relying on the *magnitude* of the BOLD response, on the other hand, cannot reveal such precise discrimination (the spatial

precision of magnitude-based fMRI has improved dramatically in recent years (Wandell, 1999; Wandell, Brewer, & Dougherty, 2005), but is still, at best, several times more coarse than that reported here). More importantly, the *magnitude* of the BOLD response is much harder to interpret; it is clear that the BOLD signal has many sources, and does not simply reflect neural excitation (it correlates with excitation, but far from perfectly). Therefore, vision scientists, and neuroscientists in general, should consider switching from magnitude based fMRI to pattern based approaches, as these are more agnostic about the underlying source of the BOLD response and are better able to reveal stimulus-based discrimination functions.

4.2. Resolving tiny displacements

The novel method here—correlating spatial patterns of retinotopic activity—successfully discriminated the positions of objects separated by about 0.24 deg. Sereno et al.'s (1995) estimate of human cortical magnification, defined as the number of millimeters cortex per degree visual angle (Daniel & Whitteridge, 1961), is $f(x) = [20.5(x + 0.08^{-1.26})]$, where x is the eccentricity of the moving Gabors in our experiment (10.89 deg). The equivalent cortical distance of this 0.24 deg separation is ~0.25 mm. Other estimates of the cortical magnification factor (Cowey & Rolls, 1974; Duncan & Boynton, 2003; Engel, Glover, & Wandell, 1997; Grusser, 1995; Sereno et al., 1995) yield consistent values between 0.2 and 0.35 mm of cortex. Therefore, our method is able to resolve sub-millimeter shifts in population activity even at large eccentricities. In fact, the spatial resolution of our technique is about as precise as the psychophysical discrimination of the Gabor positions (Fig. 1D and E). This suggests that the spatial resolution of our data is constrained primarily by the limits of the visual system, not the limits of the hardware.

Although the spatial resolution of the raw fMRI signal is coarse (in our experiment $1.5 \times 1.5 \times 2.5$ mm voxels), and there is a substantial blur added to the signal at several levels, we can measure very small changes in the profile of activity by comparing patterns of responses. In fact, it is the blurring and pooling of responses itself that contributes to such precise measurements. The same principle holds for visually perceived location as well (Regan, 2000). The positions of blurred objects can be discriminated even when misaligned by a tiny fraction of the standard deviation of the objects' contrast envelopes (Burr, McKee, & Morrone, 2005; Levi & Klein, 1990; Watt & Morgan, 1985) and even when the separation between the objects is smaller than the separation between photoreceptors (i.e., hyperacuity; Regan, 2000; Westheimer & McKee, 1977a; Westheimer & McKee, 1977b). It is worth noting that blurred stimuli are not necessary; in separate experiments, we confirmed that our spatial correlation technique can discriminate the positions of both sharp-edged and blurred objects with about the same precision (just as psychophysical discrimination of both blurred and sharp edged objects is precise; Regan, 2000; Whitaker et al., 1996).

The results demonstrate that the coded location of an object does not correspond to the peak response in the visual cortex. Although the peak contrast remained fixed in the Gabors with skewed envelopes, the population response distinguished these stimuli based on the shape of their contrast envelope. Moreover, even though the drifting Gabors may have overlapping peak activations (Ashida & Smith, 2005; Koyama et al., 2005; Liu et al., 2004; Whitney et al., 2003), the activity at the edges of the objects carry enough information to cause the population response to distinguish the drifting patterns as being shifted in position. That is, the population response classified the drifting patterns as having distinct distributions of activity depending on their direction of motion. Given that the perceived position of an object often follows the contrast profile (Watt et al., 1983; Westheimer & McKee, 1977a; Whitaker et al., 1996), it may not be surprising that the coded locations of the skewed Gabors depended on the contrast profile. That is precisely the issue, however: while the contrast profile is believed to be important for perceptual localization, the neuroimaging literature has largely neglected this; voxels that display the strongest response are routinely assumed to be most important while voxels with a weaker response—although contributing to the pattern of activity—are neglected. Approaches that localize stimulus-specific activity (either retinotopically or not) by examining patterns of responses (rather than simply peak responses) are less likely to inadvertently neglect meaningful signals (e.g., Haxby et al., 2001; Haynes & Rees, 2005; Kamitani & Tong, 2005).

5. Conclusions

The goals of the experiments here were twofold. First, we developed a new and surprisingly sensitive technique that measured the discrimination of object position based on the spatial pattern of activity (populations of voxels). We found that objects separated by as little as 0.25 deg (0.25 mm cortex) could be reliably discriminated based on the pattern of responses. This technique could be easily extended into other areas of imaging research, beyond basic retinotopy and position coding (even beyond fMRI). Second, we found that the coded location of objects in the visual cortex is not simply carried by the peak response. Rather, the entire pattern—the envelope—of activity carries meaningful information about object position.

References

Alexander, R. A., Scozzaro, M. J., & Borodkin, L. J. (1989). Statistical and empirical examination of the chi-square test for homogeneity of correlations in meta-analysis. *Psychological Bulletin, 106*, 329–331.

Allman, J., Miezin, F., & McGuinness, E. (1985). Stimulus specific responses from beyond the classical receptive field: neurophysiological mechanisms for local-global comparisons in visual neurons. *Annual Review of Neuroscience, 8*, 407–430.

Ashida, H., & Smith, A. T. (2005). Retinotopic mapping of motion stimuli in human visual cortex. *Vision Sciences Society* (5). Sarasota, FL: Journal of Vision.

Attwell, D., & Iadecola, C. (2002). The neural basis of functional brain imaging signals. *Trends Neurosciences, 25*(12), 621–625.

Bex, P. J., Edgar, G. K., & Smith, A. T. (1995). Sharpening of drifting, blurred images. *Vision Research, 35*(18), 2539–2546.

Burr, D. C., Fiorentini, A., & Morrone, C. (1998). Reaction time to motion onset of luminance and chromatic gratings is determined by perceived speed. *Vision Research, 38*(23), 3681–3690.

Burr, D., McKee, S., & Morrone, C. M. (2005). Resolution for spatial segregation and spatial localization by motion signals. *Vision Research*.

Burr, D. C., Ross, J., & Morrone, M. C. (1986). Seeing objects in motion. *Proceedings of the Royal Society of London. Series B, Biological Sciences, 227*(1247), 249–265.

Caesar, K., Gold, L., & Lauritzen, M. (2003). Context sensitivity of activity-dependent increases in cerebral blood flow. *Proceedings of the National Academy of Sciences of the United States of America, 100*(7), 4239–4244, Epub 2003 Mar 4224.

Cavanaugh, J. R., Bair, W., & Movshon, J. A. (2002). Nature and interaction of signals from the receptive field center and surround in macaque V1 neurons. *Journal of Neurophysiology, 88*(5), 2530–2546.

Cohen, J. (1988). *Statistical power analysis for the behavioral sciences*. Hillsdale, NJ: Erlbaum.

Collins, D. L., Neelin, P., Peters, T. M., & Evans, A. C. (1994). Automatic 3D intersubject registration of MR volumetric data in standardized Talairach space. *Journal of Computer Assisted Tomograph, 18*(2), 192–205.

Cowey, A., & Rolls, E. T. (1974). Human cortical magnification factor and its relation to visual acuity. *Experimental Brain Research, 21*(5), 447–454.

Daniel, P. M., & Whitteridge, D. (1961). The representation of the visual field on the cerebral cortex in monkeys. *Journal of Physiology, 159*, 203–221.

De Valois, R. L., & De Valois, K. K. (1991). Vernier acuity with stationary moving Gabors. *Vision Research, 31*(9), 1619–1626.

Duncan, R. O., & Boynton, G. M. (2003). Cortical magnification within human primary visual cortex correlates with acuity thresholds. *Neuron, 38*(4), 659–671.

Durant, S., & Johnston, A. (2004). Temporal dependence of local motion induced shifts in perceived position. *Vision Research, 44*(4), 357–366.

Edelman, G. M. (1978). Group selection and phasic reentrant signaling: a theory of higher brain function. In G. M. Edelman & V. B. Mountcastle (Eds.), *The mindful brain*. Cambridge, MA: MIT Press.

Efron, B., & Tibshirani, R. (1993). *An introduction to the bootstrap*. New York: Chapman & Hall, p. xvi, 436 pp.

Engel, S. A., Glover, G. H., & Wandell, B. A. (1997). Retinotopic organization in human visual cortex and the spatial precision of functional MRI. *Cerebral Cortex, 7*(2), 181–192.

Fitzpatrick, D. (2000). Seeing beyond the receptive field in primary visual cortex. *Current Opinion in Neurobiology, 10*(4), 438–443.

Gilbert, C. D. (1998). Adult cortical dynamics. *Physiological Reviews, 78*(2), 467–485.

Grusser, O. J. (1995). Migraine phosphenes and the retino-cortical magnification factor. *Vision Research, 35*(8), 1125–1134.

Hammett, S. T. (1997). Motion blur and motion sharpening in the human visual system. *Vision Research, 37*(18), 2505–2510.

Hammett, S. T., & Bex, P. J. (1996). Motion sharpening: evidence for the addition of high spatial frequencies to the effective neural image. *Vision Research, 36*(17), 2729–2733.

Harel, N., Lee, S. P., Nagaoka, T., Kim, D. S., & Kim, S. G. (2002). Origin of negative blood oxygenation level-dependent fMRI signals. *Journal of Cerebral Blood Flow and Metabolism, 22*(8), 908–917.

Haxby, J. V., Gobbini, M. I., Furey, M. L., Ishai, A., Schouten, J. L., & Pietrini, P. (2001). Distributed and overlapping representations of faces and objects in ventral temporal cortex. *Science, 293*(5539), 2425–2430.

Haynes, J. D., & Rees, G. (2005). Predicting the orientation of invisible stimuli from activity in human primary visual cortex. *Nature Neuroscience, 8*(5), 686–691.

Hess, R. F., & Holliday, I. E. (1992). The coding of spatial position by the human visual system: effects of spatial scale and contrast. *Vision Research, 32*(6), 1085–1097.

Hubel, D. H., & Wiesel, T. N. (1962). Receptive fields, binocular interaction and functional architecture in the cat's visual cortex. *Journal of Physiology, 160*, 106–154.

Hubel, D. H., & Wiesel, T. N. (1968). Receptive fields and functional architecture of monkey striate cortex. *Journal of Physiology, 195*(1), 215–243.

Kamitani, Y., & Tong, F. (2005). Decoding the visual and subjective contents of the human brain. *Nature Neuroscience, 8*(5), 679–685.

Koyama, S., Sasaki, Y., Watanabe, T., & Tootell, R. (2003). Expanding and contracting optic flow differentially activate retinotopic visual cortex. *Society for neuroscience* (p. Program No. 438.412). New Orleans/Washington, DC: Society for Neuroscience.

Koyama, S., Sasaki, Y., Andersen, G. J., Tootell, R. B., Matsuura, M., & Watanabe, T. (2005). Separate processing of different global-motion structures in visual cortex is revealed by FMRI. *Current Biology, 15*(22), 2027–2032.

Lennie, P. (1998). Single units and visual cortical organization. *Perception, 27*(8), 889–935.

Levi, D. M., & Klein, S. A. (1990). Equivalent intrinsic blur in spatial vision. *Vision Research, 30*(12), 1971–1993.

Li, C. Y., & Li, W. (1994). Extensive integration field beyond the classical receptive field of cat's striate cortical neurons—classification and tuning properties. *Vision Research, 34*(18), 2337–2355.

Liu, J., Ress, D., Nakadomari, S. & Wandell, B.A. (2004). Stability of human V1 retinotopy measured with moving patterns. *Society for Neuroscience Abstracts* (p. 18.11.).

Maffei, L., & Fiorentini, A. (1976). The unresponsive regions of visual cortical receptive fields. *Vision Research, 16*(10), 1131–1139.

Mathiesen, C., Caesar, K., Akgoren, N., & Lauritzen, M. (1998). Modification of activity-dependent increases of cerebral blood flow by excitatory synaptic activity and spikes in rat cerebellar cortex. *Journal of Physiology, 512*(Pt 2), 555–566.

McGraw, P. V., Walsh, V., & Barrett, B. T. (2004). Motion-sensitive neurones in V5/MT modulate perceived spatial position. *Current Biology, 14*(12), 1090–1093.

McKee, S. P., & Welch, L. (1985). Sequential recruitment in the discrimination of velocity. *Journal of the Optical Society of America A, 2*(2), 243–251.

Morgan, M. J., Mather, G., Moulden, B., & Watt, R. J. (1984). Intensity-response nonlinearities and the theory of edge localization. *Vision Research, 24*(7), 713–719.

Nishida, S., & Johnston, A. (1999). Influence of motion signals on the perceived position of spatial pattern. *Nature, 397*(6720), 610–612.

Pascual-Leone, A., & Walsh, V. (2001). Fast backprojections from the motion to the primary visual area necessary for visual awareness. *Science, 292*(5516), 510–512.

Ramachandran, V. S., & Anstis, S. M. (1990). Illusory displacement of equiluminous kinetic edges. *Perception, 19*(5), 611–616.

Regan, D. (2000). *Human perception of objects: early visual processing of spatial form defined by luminance, color, texture, motion, and binocular disparity*. Sunderland, MA: Sinauer Associates, p. xxix, 577 pp., [574] p. of plates.

Sereno, M. I., Dale, A. M., Reppas, J. B., Kwong, K. K., Belliveau, J. W., Brady, T. J., et al. (1995). Borders of multiple visual areas in humans revealed by functional magnetic resonance imaging. *Science, 268*(5212), 889–893.

Snowden, R. J. (1998). Shifts in perceived position following adaptation to visual motion. *Current Biology, 8*(24), 1343–1345.

Snowden, R. J., & Braddick, O. J. (1989). Extension of displacement limits in multiple-exposure sequences of apparent motion. *Vision Research, 29*(12), 1777–1787.

Talairach, J., & Tournoux, P. (1988). *Co-planar stereotaxic atlas of the human brain: 3-dimensional proportional system: an approach to*

cerebral imaging. Stuttgart, New York: G. Thieme, Thieme Medical Publishers, pp. viii, 122.

Thomsen, K., Offenhauser, N., & Lauritzen, M. (2004). Principal neuron spiking: neither necessary nor sufficient for cerebral blood flow in rat cerebellum. *Journal of Physiology, 560*(Pt. 1), 181–189.

Verghese, P., & McKee, S. P. (2002). Predicting future motion. *Journal of Vision, 2*(5), 413–423.

Waldvogel, D., van Gelderen, P., Muellbacher, W., Ziemann, U., Immisch, I., & Hallett, M. (2000). The relative metabolic demand of inhibition and excitation. *Nature, 406*(6799), 995–998.

Wandell, B. A. (1999). Computational neuroimaging of human visual cortex. *Annual Review of Neuroscience, 22*, 145–173.

Wandell, B. A., Brewer, A. A., & Dougherty, R. F. (2005). Visual field map clusters in human cortex. *Philosophical Transactions of the Royal Society of London. Series B, Biological Sciences, 360*(1456), 693–707.

Watt, R. J., & Morgan, M. J. (1983). The recognition and representation of edge blur: evidence for spatial primitives in human vision. *Vision Research, 23*(12), 1465–1477.

Watt, R. J., & Morgan, M. J. (1985). A theory of the primitive spatial code in human vision. *Vision Research, 25*(11), 1661–1674.

Watt, R. J., Morgan, M. J., & Ward, R. M. (1983). Stimulus features that determine the visual location of a bright bar. *Investigative Ophthalmology & Vision Science, 24*(1), 66–71.

Welch, L., Macleod, D. I., & McKee, S. P. (1997). Motion interference: perturbing perceived direction. *Vision Research, 37*(19), 2725–2736.

Westheimer, G., & McKee, S. P. (1977a). Integration regions for visual hyperacuity. *Vision Research, 17*(1), 89–93.

Westheimer, G., & McKee, S. P. (1977b). Spatial configurations for visual hyperacuity. *Vision Research, 17*(8), 941–947.

Whitaker, D., McGraw, P. V., & Levi, D. M. (1997). The influence of adaptation on perceived visual location. *Vision Research, 37*(16), 2207–2216.

Whitaker, D., McGraw, P. V., Pacey, I., & Barrett, B. T. (1996). Centroid analysis predicts visual localization of first- and second-order stimuli. *Vision Research, 36*(18), 2957–2970.

Whitaker, D., McGraw, P. V., & Pearson, S. (1999). Non-veridical size perception of expanding and contracting objects. *Vision Research, 39*(18), 2999–3009.

Whitney, D. (2002). The influence of visual motion on perceived position. *Trends in Cognitive Sciences, 6*(5), 211–216.

Whitney, D., & Cavanagh, P. (2000). Motion distorts visual space: shifting the perceived position of remote stationary objects. *Nature Neuroscience, 3*(9), 954–959.

Whitney, D., Goltz, H. C., Thomas, C. G., Gati, J. S., Menon, R. S., & Goodale, M. A. (2003). Flexible retinotopy: motion-dependent position coding in the visual cortex. *Science, 302*(5646), 878–881, Epub 2003 Sep 2018.

Zeki, S. (1990). The motion pathways of the visual cortex. In C. Blakemore (Ed.), *Vision: Coding and efficiency* (pp. 321–345). Cambridge: Cambridge University Press.